Cerebral Cortex, 2017; 1–17

doi: 10.1093/cercor/bhx175
Original Article

ORIGINAL ARTICLE

A New Modular Brain Organization of the BOLD Signal during Natural Vision

DoHyun Kim[1], Kendrick Kay[2], Gordon L. Shulman[3] and Maurizio Corbetta[3,4,5,6,7]

[1]Washington University in St. Louis, Saint Louis, MO 63110, USA, [2]Department of Radiology, University of Minnesota, Twin Cities, MN 55455, USA, [3]Department of Neurology, Washington University School of Medicine, Saint Louis, MO 63110, USA, [4]Department of Radiology, Washington University School of Medicine, Saint Louis, MO 63110, USA, [5]Department of Anatomy and Neurobiology, Washington University School of Medicine, Saint Louis, MO 63110, USA, [6]Department of Neuroscience, University of Padua, 35122 Padova, Italy and [7]Padua Neuroscience Center (PNC), University of Padua, 35122 Padova, Italy

Address correspondence to Maurizio Corbetta. Email: mcorbetta@wustl.edu; Gordon Shulman. Email: gshulman@wustl.edu

Abstract

The resting blood oxygen level-dependent (BOLD) signal is synchronized in large-scale brain networks (resting-state networks, RSNs) defined by interregional temporal correlations (functional connectivity, FC). RSNs are thought to place strong constraints on task-evoked processing since they largely match the networks observed during task performance. However, this result may simply reflect the presence of spontaneous activity during both rest and task. Here, we examined the BOLD network structure of natural vision, as simulated by viewing of movies, using procedures that minimized the contribution of spontaneous activity. We found that the correlation between resting and movie-evoked FC ($\rho = 0.60$) was lower than previously reported. Hierarchical clustering and graph-theory analyses indicated a well-defined network structure during natural vision that differed from the resting structure, and emphasized functional groupings adaptive for natural vision. The visual network merged with a network for navigation, scene analysis, and scene memory. Conversely, the dorsal attention network was split and reintegrated into 2 groupings likely related to vision/scene and sound/action processing. Finally, higher order groupings from the clustering analysis combined internally directed and externally directed RSNs violating the large-scale distinction that governs resting-state organization. We conclude that the BOLD FC evoked by natural vision is only partly constrained by the resting network structure.

Key words: BOLD, fMRI, intersubject functional correlation (ISFC), natural viewing, resting-state functional connectivity (rs-FC)

Introduction

Recent evidence indicates that spontaneous activity in the brain is not random, as traditionally modeled based on the variability of sensory response to identical stimuli, but is systematically organized as spatial patterns of temporally correlated activity (from neurons to whole brain networks) (Tsodyks et al. 1999; Varela et al. 2001; Fiser et al. 2004; Fox et al. 2005; He et al. 2008; Nir et al. 2008; de Pasquale et al. 2010; Berkes et al. 2011; Brookes et al. 2011; Florin and Baillet 2015). In fMRI studies, for example, the spatial topography of interregional temporal correlations (functional connectivity, FC) of the blood oxygen level-dependent (BOLD) signal at rest, that is, in the absence of any stimulation or task, is well described by a relatively small number of spatio-temporal clusters or networks (so-called resting-state networks, RSNs). Interestingly, the topography of BOLD RSNs is very similar to the topographies of BOLD task

activity evoked by different sensory, motor, and cognitive tasks and the FC measured during those tasks (Biswal et al. 1995; Smith et al. 2009; Mennes et al. 2013; Cole et al. 2014).

One explanation for this task-rest correspondence is that task states have been sculpted into the brain by evolution, development, and experience (Fiser et al. 2004; Albert et al. 2009; Hasson et al. 2009; Lewis et al. 2009; Tambini et al. 2010; Raichle 2011; Petersen and Sporns 2015). On this view, specific tasks represent different subsets of the repertoire of states that the brain explores at rest (Kenet et al. 2003). As a result, the neural activity that enables adaptive behavior during tasks is strongly constrained by the activity observed at rest. However, if similar sources of intrinsic activity are present at rest and during tasks, similar FC matrices will be observed for both states even if task-evoked FC is very different than resting FC. In line with this view, several authors have proposed that rest states represent a default or idling state from which many different task states can be generated through unknown mechanisms (Betti et al. 2013; Spadone et al. 2015). Therefore, the FC from adaptive neural activity, that is, activity evoked by a task, may be largely unrelated to resting FC. The first but not second view predicts that task and resting BOLD FC will be similar even if the influence of intrinsic activity during a task is removed.

In this study, we compared the topography of resting-state patterns of FC to the topography induced by natural vision, as simulated by viewing a series of short movies. Importantly, this comparison occurred after isolating the movie-evoked component free of any ongoing spontaneous or intrinsic activity, insuring that task-rest correspondences did not simply reflect the presence of intrinsic activity during both. One approach to removing intrinsic activity is to average BOLD time series across subjects, on the assumption that ongoing spontaneous activity in different subjects is not temporally synchronized. However, Henrikkson et al. reported that the effects of intrinsic activity on representational dissimilarity matrices were only partly removed by averaging BOLD time series across subjects (Henriksson et al. 2015). A different approach, called intersubject functional correlation (ISFC), was recently reported (Simony et al. 2016) (see also Mantini et al. 2012). To compute the FC between regions A and B, the BOLD time series from region A was averaged over one group of subjects, the BOLD time series from region B was averaged over a separate group of subjects, and then the time series for regions A and B was correlated.

In the first part of this paper, we show that the ISFC procedure eliminates intrinsic signals more effectively than simple averaging of time series across subjects within a group, but that at large sample sizes the 2 methods yield very similar results. We then use the ISFC procedure to show that the correlation between FC matrices for natural vision and rest is lower than previously reported. This result indicates that BOLD task-rest correspondences have been overestimated due to the common presence of intrinsic activity. Finally, by applying hierarchical clustering and graph-based analyses to the resting and movie-evoked FC matrices, we show that natural vision induces a modular network organization of the BOLD signal that differs from the organization at rest.

Methods

Human Connectome Project Data

Seventy participants (28 male, age 22–35, including pairs of identical twins) were obtained from the Washington University-Minnesota Consortium Human Connectome Project (WU-Minn HCP Data—900 Subjects + 7 T; June 2016) (Van Essen et al. 2012). BOLD signals were acquired in 2 consecutive days of experiments on a 7 T scanner (SC72 gradient coil 70–100 mT/m, multiband factor of 5, time echo = 22 ms, time repetition = 1 s, 1.6 mm voxel size) installed at the University of Minnesota (Uğurbil et al. 2013). On the first day, participants were scanned while maintaining fixation on a black screen for 2 scans, each 15 min in duration (resting state). Next, participants were scanned while watching movie clips for 2 scans, each 15 min in duration (movie task). Each movie-watching scan contained 3 to 4 short movie clips with a repeated short clip for validation of possible regression models inserted at the end of each movie session. A 20-s period of fixation on a black screen was inserted prior to the first movie clip, in between movie clips, and following the last movie clip. The same procedure was repeated for the second day. Two of the movie sessions were composed of short clip compilations of 3 Hollywood movies with short intermissions, and the other 2 movie sessions were composed of short clip compilations of 4 independent films with short intermissions (see Supplementary Fig. S1 for descriptions of movie clips).

Preprocessing

Spatial image preprocessing initially followed the HCP minimal preprocessing pipeline, minimizing spatial smoothing and spatial distortion while maximizing alignment across image modalities. The HCP minimal preprocessing pipeline transformed the data from the original resolution to 2 mm resolution into a 91 282 grayordinate space called CIFTI (Glasser et al. 2013). CIFTI grayordinates comprise cortical gray matter surface vertices (both left and right hemisphere, 30K vertices each) and subcortical gray matter voxels (30K voxels). In this study, only cortical gray matter surface vertices of both hemispheres were used.

The BOLD time series then underwent 4 additional steps. First, the data were normalized by their mean, transforming each time series into % BOLD fluctuation, and global signal regression was conducted. Second, to minimize the effect of subject motion, BOLD time series were censored and corrected using the DVARS measure (temporal derivative of RMS variance), which is highly correlated with frame-wise head-motion displacement (Power et al. 2012). For each subject, approximately 5% of BOLD frames were replaced by interpolating the magnitude values of neighboring BOLD time points.

Third, each subject's BOLD time series of cortical gray matter surface vertices (both left and right hemisphere, 30K vertices each) were registered into the Gordon–Laumann parcellation (Gordon et al. 2016), and then averaged across the vertices within a parcel. This procedure resulted in a mean BOLD time series for each parcel, reducing 60K time series to 324. The 324 Gordon–Laumann parcels are grouped into 13 different RSNs (see Supplementary Fig. S2): Visual (VIS), Retrosplenial Temporal (RST), Dorsal Attention (DAN), Dorsal Somatomotor (SMd), Somatomotor Mouth (SMv), Auditory (AUD), Cingulo-Operculum (CON), Ventral Attention (VAN), Salience (SAL), Cingulo-parietal (CPN), Fronto-parietal (FPN), Default Mode (DMN), and None. Therefore, the use of the mean parcel BOLD time series allowed simple comparisons of the functional topographies between resting-state BOLD and movie-watching BOLD while increasing the signal-to-noise ratio of movie-evoked and resting BOLD time series.

The final processing step was temporal filtering of the mean parcel BOLD time series. Since low-frequency fluctuations (<0.1 Hz) account for about 90% of the correlation coefficient between regions, a bandpass filter of 0.008–0.08 Hz was applied (Cordes et al. 2001). For each movie BOLD time series, the first

6 s from the beginning of each clip within each movie was eliminated to account for hemodynamic lag.

Resting-State Functional Connectivity and Movie Functional Connectivity

BOLD signal time series obtained from different scans were concatenated, and a correlation matrix was computed for each subject by calculating parcel-to-parcel, that is, pairwise, the temporal correlation (Pearson *r*) between time series. Pearson *r*-values for individual parcel pairs were converted to Fisher z-transformed values. A group average rs-FC matrix was obtained by averaging over subjects the individual subject correlation matrices and then transforming the Fisher z-values into Pearson *r*-values (Fig. 1, left).

FC after Temporal Averaging: Movie and Resting State

Temporal averaging time-locked to specific events is used in neurophysiology to increase signal to noise of stimulus or task-evoked activity. Previous work has shown that movie observation leads to highly synchronized signal time series across different subjects, due presumably to consistent phase resets of ongoing spontaneous activity induced by events in the movie (Hasson et al. 2004; Mantini et al. 2012). Therefore, averaging across subjects BOLD time series from a specific parcel prior to computing FC should lead to suppression of correlations due to intrinsic activity and subject-specific movie-evoked activity, and should enhance the correlation due to movie-evoked activity shared across subjects. We computed parcel-to-parcel FC matrices on group-averaged BOLD signal time series in the resting state (rs-avgFC) and during the movie (m-avgFC) (Fig. 1, middle). The prediction is that movie FC should reflect predominantly movie-related activity shared across subjects, whereas resting-state FC should show weak or no correlation because intrinsic activity should not be synchronized across subjects.

Intersubject Functional Correlation

The effectiveness of temporal averaging in removing effects of intrinsic activity on FC was compared with that of a second method, "ISFC," which was recently introduced by Simony et al. (2016)

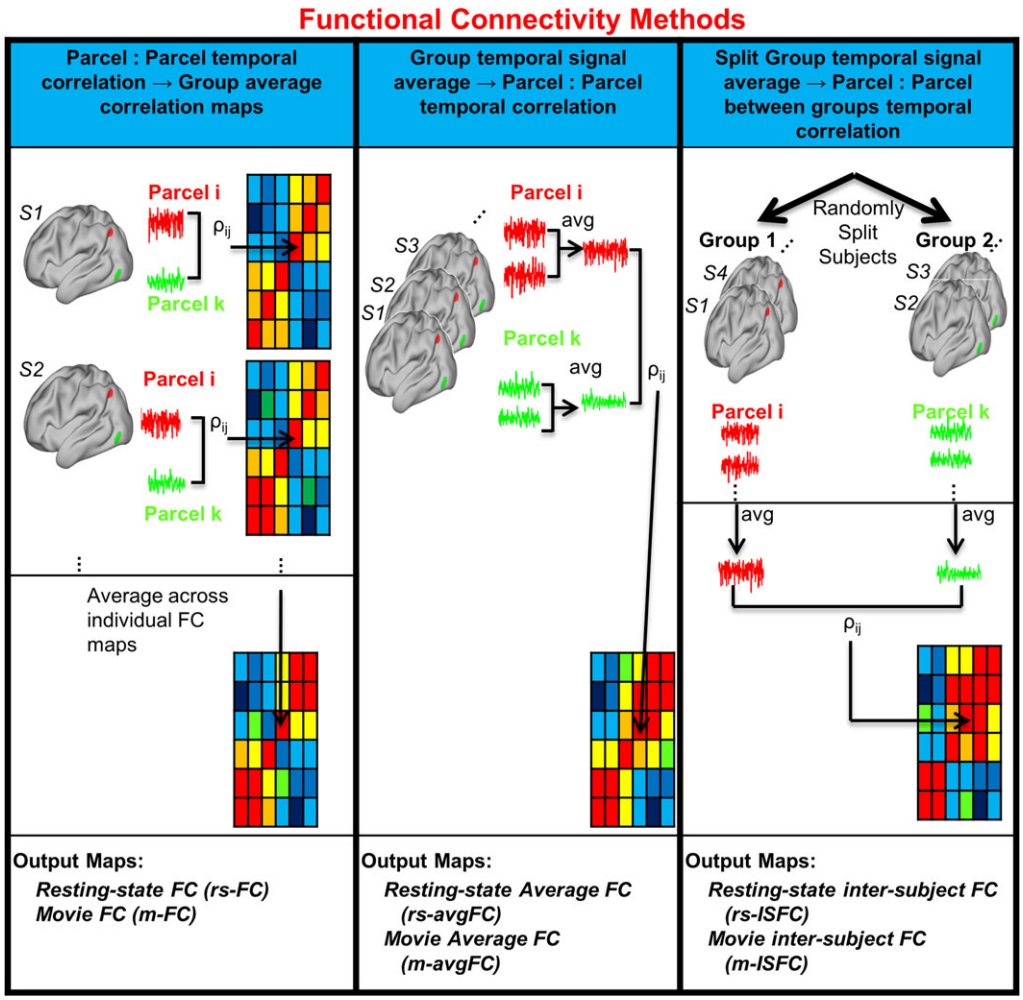

Figure 1. Three methods for computing FC matrices. (Left) rs-FC and movie FC (m-FC) group correlation matrices were generated by averaging individual correlation matrices that were computed from pairwise, parcel-to-parcel BOLD temporal correlations. (Middle) For both movie and resting-state conditions, the BOLD time series for each parcel was first temporally averaged across subjects. Then, group m-avgFC and rs-avgFC matrices were calculated from pairwise, parcel-to-parcel BOLD temporal correlations. (Right) In the ISFC method, subjects were randomly split into 2 groups. Within a group, the BOLD time series for each parcel was first temporally averaged across subjects. Then, a group FC matrix was computed by correlating, for each pair of parcels, the parcel time series from one group with the parcel time series from the other group. This procedure was repeated fifty times with different random groupings of subjects, and the resulting FC matrices were averaged to produce the final group m-ISFC and rs-ISFC matrices.

(see also Mantini et al. 2012). Subjects were evenly and randomly split into 2 groups. For each parcel, the BOLD signal time series were averaged across the subjects within each group. Then a parcel-by-parcel pairwise FC matrix was computed between groups. The computed FC was not symmetric at this point since the correlation coefficients of paired region A and B were computed as:

$$\rho_{AB,\ \text{upper diagonal}} = \text{correlation between the BOLD (region A, Group 1) and BOLD (region B, Group 2).}$$
$$\rho_{BA,\ \text{lower diagonal}} = \text{correlation between the BOLD (region A, Group 2) and BOLD (region B, Group 1).}$$

To keep the conventional unidirectional connectivity characteristic of FC, symmetricity in ISFC was imposed by averaging upper-diagonal values and lower diagonal values. By randomly permuting 50 times the subjects assigned to each group, 50 FC matrices were obtained. The *r*-values of the 50 matrices were converted to Fisher z-transformed values, the 50 matrices were averaged, and the values of the averaged matrix were converted from z-values back to *r*-values (Fig. 1, right). ISFC matrices were computed for both resting-state and movie-evoked time series.

Statistical Analysis of Time Series Correlations

The statistical significance of each observed correlation was accessed by a permutation procedure based on surrogate data (Simony et al. 2016). Phase-randomized surrogate BOLDs time series of equal mean and autocorrelation to the original signal were obtained. The phase-randomization was computed by rotating the phase $\phi(f)$ by an independent random variable $\varphi(f)$ which was uniformly chosen in the range of $[0, 2\pi)$ (Prichard and Theiler 1994).

For the orthogonality test, null distributions of both maximum noise correlation values and minimum noise correlation values were obtained via repeated generations (1000) of surrogate BOLD signals (Resting-state, movie-evoked, and movie-residual). FWER were controlled by a threshold (R^*) at the q^*100th percentile of the null distribution of maximum values. The thresholds for each conditions are given above in each case (all for $q < 0.005$), along with the % significant ROI pairs out of the 52 326 possible ROI pairs.

For each surrogate resting-state BOLD and movie BOLD, all FC maps (rs-FC, rs-avgFC, rs-ISFC, m-FC, m-avgFC, and m-ISFC) were computed, then the maximum noise correlation values and the minimum noise correlation values for each FC map were obtained. By repeating the above procedure 5000 times, null distributions of the maximum noise correlation values and the minimum noise correlation values were obtained for each FC map. Family-wise error rate (FWER) was controlled by a threshold (R^*) at the q^*100th percentile of the null distribution of maximum values ($q = 0.005$). Since separate thresholds were applied for positive and negative values, the FWER was 0.01, 2-tailed.

Data-Driven FC Network Reorganization

The resting-state (rs-FC) and movie-evoked (m-ISFC) FC matrices generated above were organized in terms of the predefined RSNs. To analyze the network organization of the resting-state and movie-evoked state, 3 different unsupervised, data-driven analyses were conducted.

First, hierarchical clustering methods were implemented. Resting-state (rs-FC) and movie-evoked (m-ISFC) FC matrices were converted to dissimilarity matrices by calculating a dissimilarity index (1 – Pearson's *r* for paired parcels). A hierarchical clustering analysis, applied to each matrix, yielded an FC dendrogram (Connolly et al. 2012; Cauda et al. 2014; Riedel et al. 2015). The number of clusters (detected communities) were determined by the Davies–Bouldin index (DBI), which determines the optimal number of clusters (Davies and Bouldin 1979). FC matrices were then reordered based on the hierarchical clustering results.

Second, resting-state FC (rs-FC) and movie-evoked FC (m-ISFC) were reorganized into communities by implementing the Louvain community detection algorithm (Blondel et al. 2008) from the Brain Connectivity Toolbox (Rubinov and Sporns 2010) for varying threshold edge densities (4–20%). Due to the randomized initialization procedure, each run of algorithm resulted variations in detected communities. To account these variations, 10 000 runs of Louvain algorithms were conducted for each FC maps. For each parcel, the most frequently assigned community throughout the entire iterations was chosen. For the network modularity measurement, the average modularity across runs of algorithm was used. To evaluate the stability of communities, Newman's Q modularity (Newman 2004) was evaluated based on both newly detected communities (unsupervised) and predefined RSNs (supervised). The values of modularity ranges between 0 (community is no better than random connection) and 1 (strong community structure) while the modularity of typical networks with a strong modular structure ranges from 0.3 to 0.7 (Newman and Girvan 2004). Since movie-evoked FC (m-ISFC) was an averaged map of 50 different permutations of split subjects, the modularity scores were assessed for each permutation. Similarly, the modularity scores of resting-state FC (rs-FC) were assessed from 50 different permutations of rs-FC generated from 35 randomly chosen subjects. To test for a difference in mean modularity scores between rs-FC and m-ISFC, a cluster-based nonparametric test with a *P*-value of 0.0001 was performed (Maris and Oostenveld 2007) as follows:

1. Collect trials of the 2 experimental conditions (the modularity scores of rs-FC and m-ISFC in all permutations).
2. Draw a combined dataset that had 2 subsets of randomly assigned modularity scores.
3. Calculate the difference in mean modularity scores between subsets.
4. Repeat above steps 2 and 3 1 000 000 times to construct a histogram of the difference in mean modularity scores.
5. Calculate a *P*-value based on the proportion of random partitions that resulted in a larger test statistic than the observed one.

Finally, resting-state FC (rs-FC) and movie-evoked FC (m-ISFC) were visualized with spring-embedded models that were computed using a 4% threshold edge density. Similarly, communities defined from hierarchical clustering and Louvain community detection algorithms were visualized with spring-embedded models.

Results

Orthogonality of Movie-Evoked and Resting BOLD Signals

We first checked that group-averaged BOLD signals evoked by the movie were orthogonal to intrinsic signals, since otherwise removing one signal would partly remove the other.

Two different methods were used to test orthogonality. In the first, we averaged the movie BOLD time series from 35 subjects (Group 1) to get a stable estimate of the movie-evoked BOLD time series. We then correlated this Group 1 time series with the resting-state time series of each subject from a different group of 35 subjects (Group 2). The correlation between the Group 1 (average) and Group 2 (single subject) time series was on average, essentially zero with a small standard deviation across Group 2 subjects (correlation coefficient: $\mu = -6.32e^{-4}$ and $\sigma = 0.041$). A nonparametric permutation test with family error wise correction for the significance of the computed FC (Simony et al. 2016) indicated no significant ROI pairs (threshold $R^* = -0.289$ and 0.288).

In a second analysis, we again averaged the movie BOLD time series from 35 subjects (Group 1) to get a stable estimate of the movie-evoked BOLD time series. For each subject in a different group of 35 subjects (Group 2), we subtracted the Group 1 time series from the movie time series for that Group 2 subject to yield a residual time series. The residual time series contained subject-specific movie-evoked BOLD signals and intrinsic signals, with at most a small contribution from movie-evoked signals. We then correlated the residual time series for that Group 2 subject with the Group 1 average movie-evoked time series. The correlation between the 2 time series was on average, essentially zero with a small standard deviation across Group 2 subjects (correlation coefficient: $\mu = -0.003$ and $\sigma = 0.057$). A total of 0.31% of significant ROI pairs were found (threshold $R^* = -0.282$ and 0.282).

The above analyses show that the group movie-evoked BOLD signal is orthogonal to the resting-state and movie-residual BOLD signals. We also conducted 2 tests of the orthogonality of different resting-state time series. In the first analysis, we correlated the resting BOLD time series across runs within a subject. The correlation between 2 time series was on average, essentially zero with a small standard deviation across subjects (correlation coefficient: $\mu = -0.001$ and $\sigma = 0.060$), and no significant ROI pairs were found (threshold $R^* = -0.292$ and 0.291). In a second analysis, we correlated the resting-state BOLD time series from different subjects for a given run. Again, the correlation between the 2 time series was on average, essentially zero with a small standard deviation across subjects (correlation coefficient: $\mu = -4.16e^{-4}$ and $\sigma = 0.041$). No significant ROI pairs were found (threshold $R^* = -0.217$ and 0.221).

The Influence of Intrinsic Activity on Network Synchronization during Natural Vision

Because the BOLD signal measured during movie viewing includes both intrinsic fluctuations and movie-evoked fluctuations (Fox et al. 2006; Becker et al. 2011), pure movie-evoked patterns of interregional signal synchronization can only be isolated after removing the fluctuations due to intrinsic activity. We tested 2 procedures for accomplishing this.

Figure 2*a* shows the group resting FC matrix (rs-FC), which was computed by averaging across subjects the single-subject FC matrices formed from the correlations between BOLD time series for all pairs of parcels from the Gordon–Laumann parcellation (see Fig. 1, left panel). The rs-FC matrix shows the characteristic block structure along the diagonal that highlights different RSNs. A nonparametric test (FWER $P = 0.01$, 2-tailed) indicated that 84.7% of ROI pairs in the rs-FC matrix were significant. Figure 2*d* shows the group movie FC matrix (m-FC), similarly computed by averaging of single-subject FC matrices computed from the BOLD time series during movie viewing. A nonparametric test (FWER $P = 0.01$, 2-tailed) showed that 82.0% of ROI pairs in the m-FC matrix were significant. The spatial correlation between the resting and movie FC matrices was very high, 0.87, replicating the correspondence between task and rest FC previously reported (Cole et al. 2014). However, this correspondence may have reflected the common influence of intrinsic activity. To compute pure movie-evoked FC, we averaged the BOLD time series from different parcels over subjects before computing the FC between parcels (see Fig. 1, middle panel). Since fluctuations of intrinsic activity vary in time from subject to subject, intersubject averaging of BOLD time series should reduce the magnitude of intrinsic BOLD variation to near zero, leaving only the components that are time-locked to events in the movie. The movie-evoked FC after intersubject averaging (m-avgFC) is shown in Figure 2*e*. A nonparametric test (FWER $P = 0.01$, 2-tailed) showed that 38.2% of ROI pairs in the m-avgFC matrix were significant. The spatial correlation between resting and movie-evoked matrices was only 0.63, much less than the previous correlation (0.87), consistent with a reduction of the large contribution of intrinsic activity.

To test whether the intersubject averaging procedure completely removed the effect of intrinsic activity on FC, we applied the same procedure to the resting-state data. After intersubject averaging, each parcel's BOLD time series showed only small variations around zero, as expected (not shown). Nevertheless, as shown in Figure 2*b*, the resulting FC matrix (rs-avgFC) was almost identical to the original resting FC matrix, with a spatial correlation of 0.95. Therefore, the influence of intrinsic activity on the topography of movie-evoked FC was not fully removed by intersubject averaging of parcel BOLD time series. This result is consistent with a recent report that averaging of BOLD time series during natural image viewing is insufficient to remove intrinsic fluctuations (Henriksson et al. 2015). A nonparametric test (FWER $P = 0.01$, 2-tailed) showed that 13.6% of ROI pairs in the rs-avgFC matrix were significant.

ISFC Effectively Removes the Influence of Intrinsic Activity

We tested a second procedure for removing intrinsic activity called "ISFC" (see Fig. 1, right panel), which was recently introduced by Simony et al. (2016). Briefly, the method involves the same assumption as the first method, namely that intrinsic activities are uncorrelated across subjects. However, intrinsic activity is removed by correlating the BOLD time series for 2 parcels across 2 groups of subjects rather than within the same group. First, subjects were randomly split into 2 groups. Then, the BOLD time series for each parcel was averaged within each group, similar to the intersubject averaging procedure of the first method, resulting in a relatively stable estimate of the movie activity for each parcel. Note, however, that since data from only half of the subjects were used to compute the average time series in a group, the parcel time series for the ISFC method had lower signal-to-noise than the time series computed using the intersubject averaging method. In the final step of the ISFC method, we computed the FC between 2 parcels by correlating the averaged time series for the first parcel from one group with the averaged time series for the other parcel from the other group. This correlation step was repeated for all pairs of parcels to derive a complete FC matrix. The same procedure was then repeated over many iterations using different assignments of subjects to the 2 groups. A final ISFC matrix was computed by averaging the matrices generated from each iteration.

The FC matrix computed by applying the ISFC procedure to the resting-state scans (rs-ISFC) is shown in Figure 2c. No structure is evident, with the correlations tightly grouped around zero (mean correlation $\rho = 3.57e{-}4$, $\sigma = 0.03$, max $\rho = 0.12$, min $\rho = -0.13$). A nonparametric test (FWER $P = 0.01$, 2-tailed) showed that no ROI pairs in the rs-ISFC matrix were significant. Moreover, the spatial correlation between the rs-ISFC matrix and the original resting-state matrix (rs-FC) was only 0.10. These results indicate that the effects of intrinsic activity on FC were more fully removed by the ISFC than intersubject averaging procedure.

Finally, we computed movie-evoked FC using the ISFC procedure (Fig. 2f, m-ISFC), allowing us to determine pure movie-evoked FC free of any influence from intrinsic activity. The overall topography of the m-ISFC matrix was very similar to that of the m-avgFC matrix. A nonparametric test (FWER $P = 0.01$, 2-tailed) showed that 61.2% of ROI pairs in the m-ISFC matrix were significant. Correspondingly, the correlation between the m-ISFC and rs-FC matrices was 0.60, only slightly less than the correlation (0.63) between the m-avgFC and rs-FC matrices. Therefore, the ISFC and intersubject averaging methods produced very similar movie-evoked FC matrices, even though they produced very different resting FC matrices. The reasons for this discrepancy are considered in the discussion.

Intersubject Averaging was More Contaminated by Intrinsic Activity when FC was Computed from Fewer Subjects

The preceding section demonstrated that the ISFC method more fully removed the influence of intrinsic activity during movie-watching than the intersubject averaging method. We next determined the effectiveness of each method as a function of the number of subjects used to compute the FC matrices, since as a practical matter, large datasets may not be routinely available.

Spatial correlations between different FC matrices as a function of the number of subjects are illustrated in Figure 3 (see Supplementary Figs S3–S5 for the FC matrices for $N = 10$, 20, and 40 subjects). The effectiveness of the ISFC procedure in removing intrinsic activity is depicted in Figure 3a. Regardless of sample size, the spatial similarity of the rs-FC and rs-ISFC matrices was quite low (Fig. 3a, green), indicating that the rs-ISFC matrix contained no resting network structure. Conversely, the spatial similarity of the rs-FC and rs-avgFC matrices was quite high for all sample sizes (Fig. 3a, blue), indicating that resting network structure was preserved in spite of the averaging of resting time series across subjects.

Figure 3b compares the similarity of the topography of intrinsic activity during rest (rs-FC) with the topographies during

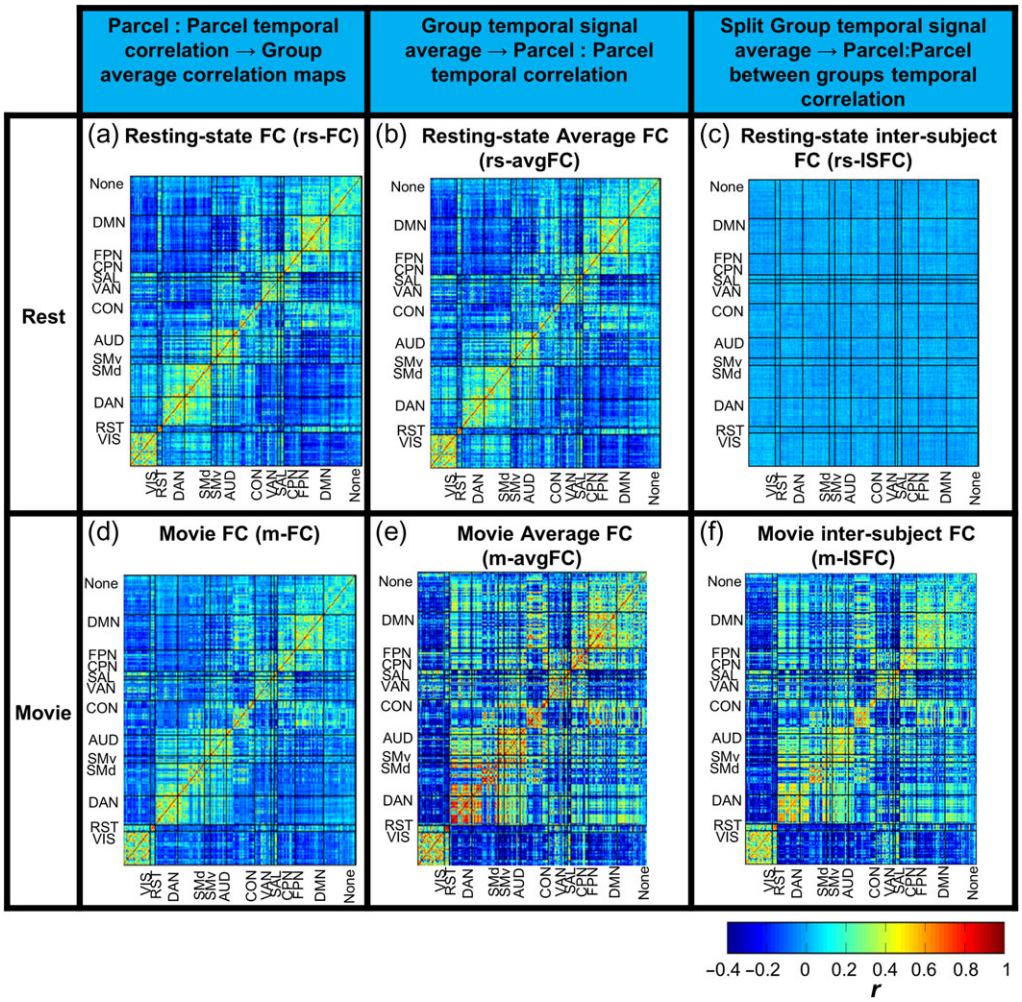

Figure 2. FC matrices for rest and natural vision generated by 3 methods. FC matrices for both resting-state BOLD and movie-watching BOLD were computed using the methods shown in Figure 1. (*a*) Resting-state FC (rs-FC), (*b*) resting-state average FC (rs-avgFC), (*c*) rs-ISFC, (*d*) movie FC (m-FC), (*e*) movie average FC (m-avgFC), and (*f*) m-ISFC.

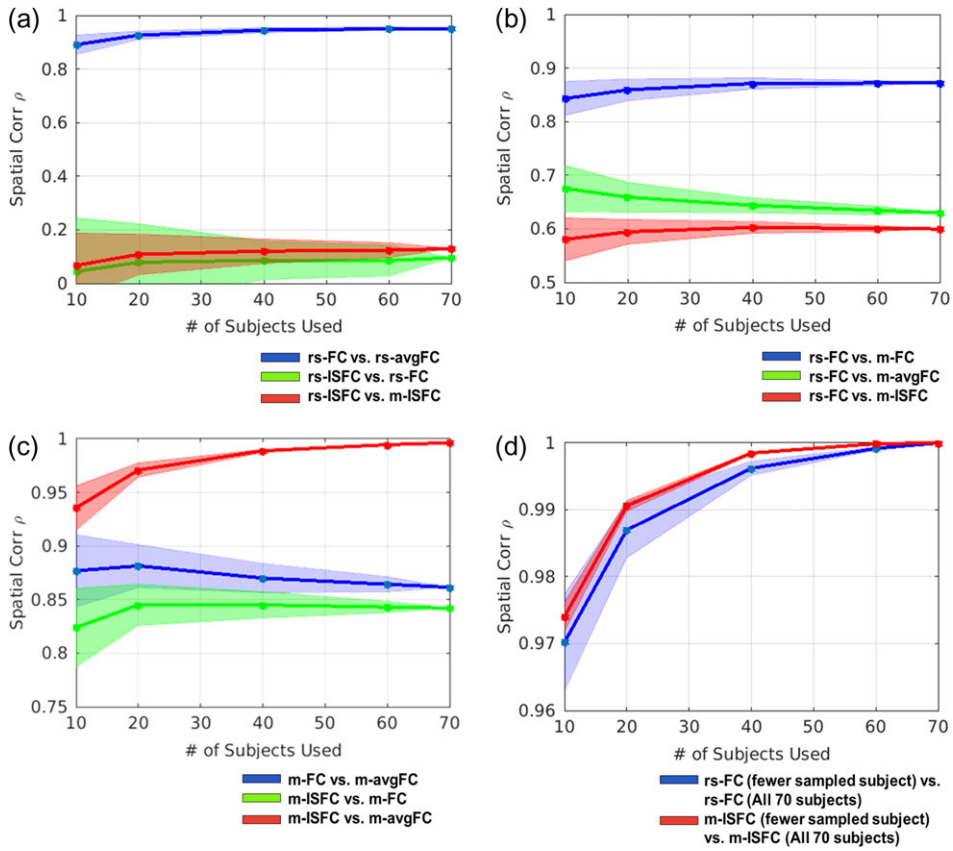

Figure 3. Spatial correlation of FC matrices as a function of sample size. (*a*) Correlation of resting-state FC (rs-FC) with resting-state average FC (blue) and resting-state intersubject FC (green), and correlation of rest and movie intersubject FC (red), with 95% confidence intervals. (*b*) Correlation of resting-state FC (rs-FC) with movie FC (m-FC, blue) movie average FC (m-avgFC, green) and movie intersubject FC (m-ISFC, red), with 95% confidence intervals. (*c*) Correlation of movie FC matrices that were computed using the 3 methods of Figure 1, with 95% confidence intervals. (*d*) FC matrices based on all 70 subjects were compared with matrices of the same type computed from fewer subjects (rs-FC, blue; m-ISFC, red), with 95% confidence intervals.

movie-watching in which intrinsic activity was left in (m-FC), was putatively removed by averaging time series over subjects (m-avgFC), or was putatively removed by computing FC between subjects (m-ISFC). Regardless of sample size, resting FC was highly correlated with movie FC when intrinsic activity was not removed (Fig. 3*b*, blue). Averaging of time series across subjects reduced rest-movie correlations (Fig. 3*b*, green), with an effect that increased signal-to-noise (movie-evoked activity to intrinsic activity) ratio at larger sample sizes, as expected. However, even at the largest sample size, the correlation of resting and movie FC was lowest with the ISFC procedure (Fig. 3*b*, red). The slight increase in the spatial similarity of the rs-FC and m-ISFC matrices (Fig. 3*b*, red) with sample size likely reflected a corresponding increase in the SNR for each parcel time series, as discussed above. Because this effect appeared to asymptote by the largest sample size, however, it likely does not explain the residual difference between the correlations of rs-FC with m-avgFC versus m-ISFC. Overall, the ISFC procedure was the most effective at removing intrinsic activity and performed well at all sample sizes. For large sample sizes, the averaging and ISFC methods yielded similar results for movie-evoked FC, but not resting FC.

The spatial similarity of the movie FC matrices computed using the 3 methods of Figure 1 was evaluated in Figure 3*c*. The high spatial correlation values between m-ISFC and m-avgFC showed that the overall topography of m-ISFC was very similar to that of m-avgFC, particularly when a sufficient number of subjects were sampled (Fig. 3*c*, red). Finally, the reliability of the ISFC procedure is shown in Figure 3*d*. The spatial correlation between m-ISFC from only 10 random subjects and m-ISFC from all 70 subjects was high (Fig. 3*d*, red), indicating that the topography of pure movie-evoked FC was captured with small samples.

Effect of Number of BOLD MR Frames on the Similarity of Rest and Movie FC Matrices

Resting and movie FC matrices are more accurately estimated as more BOLD frames are analyzed (Laumann et al. 2015). We evaluated how the spatial correlation between rs-FC and movie FC matrices depended on epoch length (number of BOLD frames) (Supplementary Fig. S6). For example, we analyzed 5 independent BOLD datasets (both movie and rest), each consisting of 500 BOLD frames, yielding 5 rs-FC, 5 m-FC, 5 m-avgFC, and 5 m-ISFC matrices. The spatial correlation among the rs-FC and movie FC matrices was computed for each of the 25 possible combinations and then averaged. Supplementary Figure S6 shows the correlation coefficient between resting and movie FC matrices as a function of the epoch length. For all movie FC matrices, the correlation with the rest FC matrix increased with epoch length, consistent with previous work (Laumann et al. 2015).

Consistency of Reductions in Task-Rest Similarity Across Movies

The similarity of task-evoked and resting FC matrices was substantially reduced when the effects of intrinsic activity on movie FC were eliminated using the ISFC procedure. We next determined whether this reduction was consistent across the movies in the HCP dataset, which differed widely in content (including Hollywood movies, documentaries, commercials, and independent movies (Supplementary Fig. S1). Consistency would suggest that the reduction in similarity did not depend on the details of the cognitive processes engaged by each movie.

Movie FC matrices (m-FC and m-ISFC) were computed for each of 12 movies that lasted at least 3 min (see Supplementary Fig. S1). The spatial correlation of each movie matrix with the resting FC matrix (rs-FC) was then measured (see Supplementary Table S1). The similarity of individual m-FC matrices to the resting FC matrices varied over a small range ($\mu = 0.80$, $\sigma = 0.032$), as did the similarity of m-ISFC matrices ($\mu = 0.48$, $\sigma = 0.028$). The lower spatial correlation value of each individual movie matrix to the resting matrix relative to the original aggregate analysis, reflected the smaller number of BOLD frames that were analyzed for each movie (e.g., for the individual m-ISFC matrices the mean correlation was 0.48 while in the aggregate analysis the correlations was 0.60; see section Effect of Number of BOLD MR Frames on the Similarity of Rest and Movie FC Matrices). Importantly, all 12 movies showed a substantial reduction in task-rest similarity when intrinsic activity was removed (see bottom row, Supplementary Table S1). Therefore, the large decreases in task-rest similarity after the removal of intrinsic activity generalized over the individual movies within the HCP dataset, indicating that the reduction did not depend on the detailed content of the movies.

Different Patterns of Functional Interactions during Rest and Natural Vision

Since the ISFC procedure effectively removed the influence of intrinsic activity on FC, we next considered the relationship between FC during rest and natural vision. The spatial correlation between the m-ISFC and rs-FC matrices was 0.60, lower than the 0.87 correlation between the m-FC and rs-FC matrices. Because the influence of intrinsic activity was removed; however, this residual similarity reflected signals generated from entirely different sources, that is, intrinsic versus movie-evoked activity.

During movie-watching (Fig. 2*f*) the FC of individual regions, relative to rest, was selectively increased or decreased with other regions in the same network, and particularly with other regions in different networks, resulting in a heterogeneous m-ISFC matrix. We statistically evaluated these within-network and between-network FC changes from rest to natural vision by measuring the mean and variance of the FC of region pairs within and across the standard resting networks. In Figure 4*a* (movie) and Figure 4*b* (resting), the diagonal and off-diagonal cells show, respectively, the mean FC of parcel pairs within each network and between each pair of networks. Figure 4*c* indicates the difference in mean FC between movie and rest, with cells showing a significant difference in mean FC displayed in color. Statistical significance was determined by *t*-tests over the different interregional FC values within a network or across networks, with a *P*-value of 0.05 after Bonferroni correction for multiple comparisons (a total of 78 comparisons, comprising the diagonal and upper-diagonal cells of the FC matrix and excluding the "none" category). Figure 4*d*–*f* shows the analogous matrices for the variance of FC, with significance determined by *F*-tests.

Not counting the cells involving the "none" category, 60.3% of the cells (47/78) showed significant differences between rest and movie in mean FC, including both increases (e.g., DAN FC) and decreases (e.g., DAN-VIS FC) in FC from rest to movie. Significant mean effects were observed in 33.3% (4/12) of within-network and 65.2% (43/66) of between-network cells. Significant differences in variance were more common overall, occurring in 79.5% (62/78) of cells, and in all cases reflected increased variance during the movie. Nonsignificant effects often involved networks that contained relatively small numbers of regions (e.g., CPN, SAL). Significant variance effects were observed in 66.7% (8/12) of within-network cells and 81.8% (54/66) of between-network cells. Therefore, significant differences in both mean FC and variance occurred in a higher percentage of between-network than within-network cells.

A New Set of Networks during Natural Vision

The statistical analysis of the FC matrices for rest and natural vision indicated that natural vision involved a large-scale reorganization of BOLD resting network structure. This reorganization could have involved the formation of a new set of networks that were just as modular as those observed during rest, or a less modular structure in which most regions broadly interacted with many other regions. To objectively identify the BOLD network organizations for intrinsic and movie-evoked FC, we conducted both hierarchical clustering analyses and graph-theory analyses of modularity and community structure on the rs-FC and m-ISFC matrices.

In order to conduct the hierarchical clustering analysis, the Pearson correlation coefficients within each FC matrix were transformed to dissimilarity indices ($d_{ij} = 1 - \rho_{ij} \parallel ij$ = pair of parcels$_i$ and parcels$_j$). The optimal number of clusters for each FC matrix ($N_{clust,rs\text{-}FC} = 2$ and $N_{clust,m\text{-}ISFC} = 7$) was determined by the DBI (Davies and Bouldin 1979), as shown in Figure 5*a*,*d*. The ordering of parcels in the rs-FC matrix was rearranged to match the dendrogram generated by the clustering analysis and is displayed in Figure 5*b*. The color assignments in the dendrogram were based on the same color assignments as the predefined networks from the Gordon–Laumann parcellation (Supplementary Fig. S1). Figure 5*b* shows that the color arrangements within the rs-FC dendrogram were mostly, although not always, homogeneous, indicating that the clustering algorithm largely replicated the apriori network structure. Moreover, the 2 clusters at the top level of the hierarchy were consistent with previous demonstrations of a large-scale distinction between externally and internally directed networks (Fox et al. 2005; Golland et al. 2008). Cluster 1 (Fig. 5*c*) included most/all parcels belonging to the RST, CON, FPN, and DMN networks, corresponding to an internal network grouping, and the second cluster included most/all parcels belong to the VIS, SMd SMv, AUD, VAN, and DAN networks, corresponding to an external network grouping. Figure 5*g* left panel shows the topography of the external and internal clusters.

The ordering of parcels in the m-ISFC matrix was also rearranged in line with the clustering analysis and is displayed in Figure 5*e*. Figure 5*f* shows the composition of 5 of the seven clusters at the top level of the hierarchy (the other 2 clusters contained only 1 and 2 parcels, and are not shown). Several results stand out. The m-ISFC matrix (Fig. 5*e*) showed a clear block structure along the main diagonal, reflecting a modular,

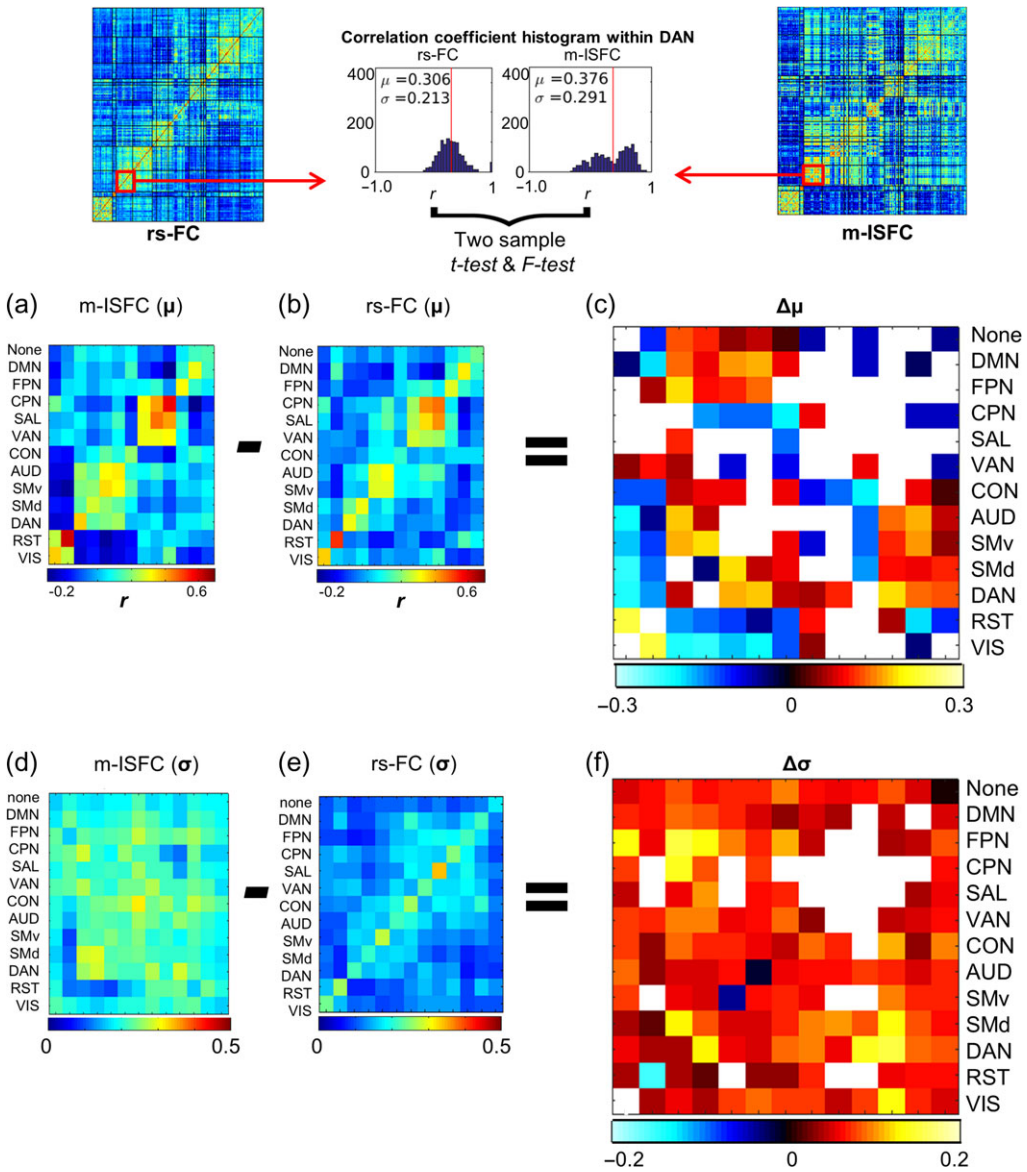

Figure 4. Statistical analysis of changes in network organization between rest and natural vision. Mean FC of region pairs within and across RSNs was computed for movie-evoked (m-ISFC, *a*) and resting-state (rs-FC, *b*) FC. The mean difference matrix (*c*, m-ISFC minus rs-FC) is depicted with cells of only significant difference in the mean of FC (as determined by *t*-tests with a *P*-value of 0.05 after Bonferroni correction for multiple comparisons, total 78 comparisons of diagonal and upper-diagonal values only, excluding the "none" category). Variance of the FC of region pairs within and across the RSNs were computed for both movie-evoked (m-ISFC, *d*) and resting-state (rs-FC, *e*) FCs. The variance difference matrix (*f*, m-ISFC minus rs-FC) is depicted with cells of only significant difference in the variance of FC (as determined by *F*-tests with a *P*-value of 0.05 after Bonferroni correction for multiple comparisons, total 78 comparisons of diagonal and upper-diagonal values only, excluding the "none" category).

network organization. However, this modular organization departed from the apriori network structure. Some apriori networks were combined largely intact to form new groupings adaptive for natural vision. Cluster #5 (Fig. 5*f*) merged a largely intact visual network with an intact RST network, which is involved in navigation, scene perception, and scene memory, along with some parcels from the fronto-parietal network. However, many apriori networks were split up and distributed across different clusters (Fig. 5*f*). For example, the DAN was split between clusters #3 and #4. Interestingly, the large-scale division between internal and external networks was not respected, with clusters including parcels from networks of both types. For example, the largest cluster in the m-ISFC matrix, cluster #3, included parcels from both external networks (e.g., SMd, AUD, DAN) and internal networks (e.g., CON, FPN, DMN). Similarly, the DBI for natural vision did not show a minimum at 2 clusters (Fig. 5*d*), unlike the index values for the resting-state (Fig. 5*a*). The topography of the 5 clusters is shown in Figure 5*g*, right. We defer a description of the possible functions associated with these clusters until further analyses are presented.

One general conclusion from the clustering analysis is that during natural vision, regions from the resting networks were redistributed into a new set of BOLD networks. This redistribution should have reduced the modularity of the m-ISFC graph computed using the apriori networks. Figure 6*a*, left panel confirms this prediction, with much lower modularity scores during natural vision than rest. However, when modularity was

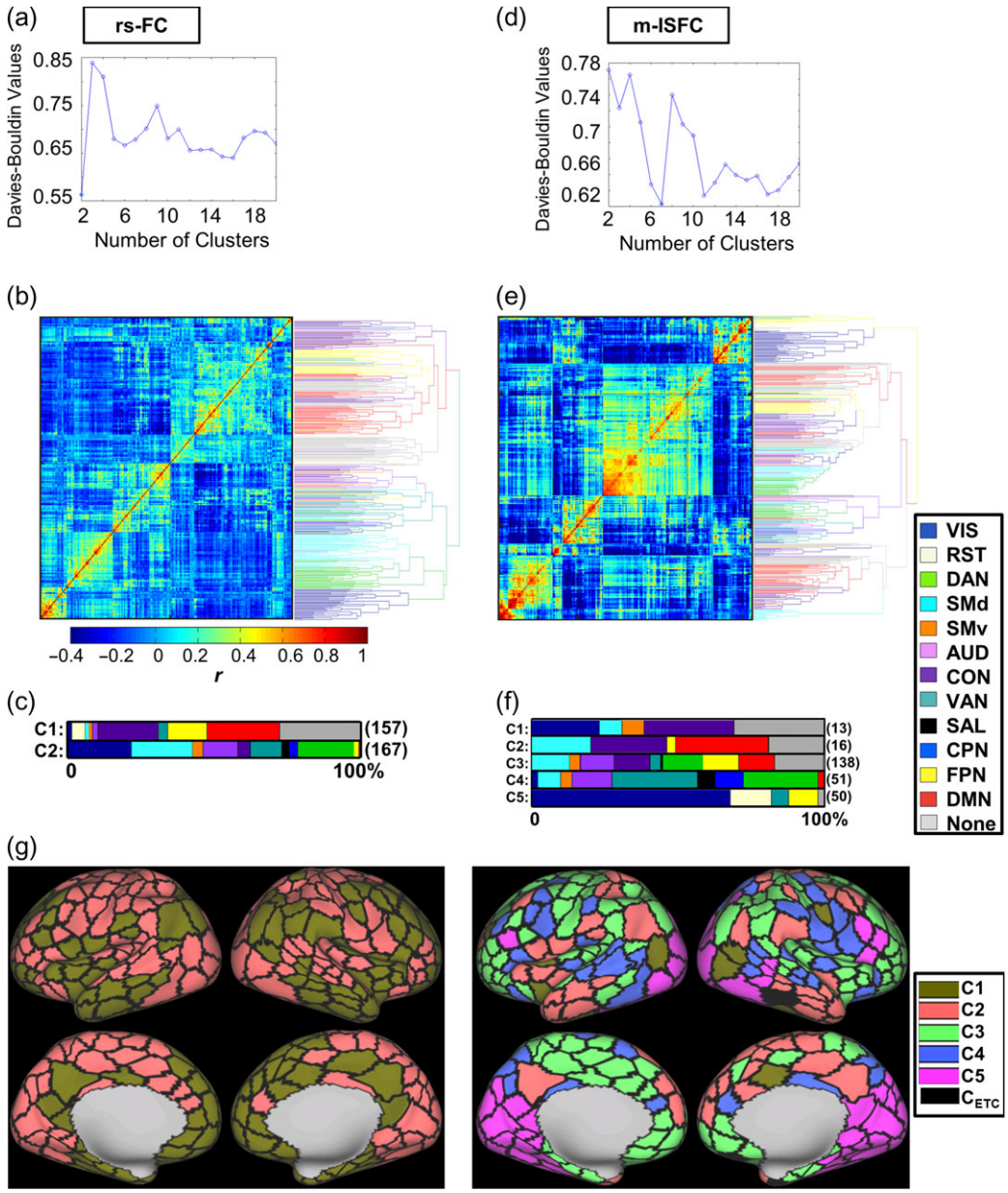

Figure 5. Hierarchical clustering analysis reveals distinctive network organizations for rest and natural vision. (*a*,*d*) DBI values as a function of the number of clusters for rs-FC (*a*, minimum DBI = 2) and m-ISFC (*d*, minimum DBI = 7). (*b*,*e*) Region labels along the x- and y-axis of the resting-state FC matrix (*b*) and m-ISFC matrix (*e*) were reordered in accordance with the dendrogram from the hierarchical clustering algorithm. The dendrogram was colored according to the predefined network assignments from the Gordon–Laumann (GL) parcellation (Supplementary Fig. S1). (*c*,*f*) Percentage distribution of predefined GL RSNs for each cluster (e.g., C1) defined from the hierarchical clustering algorithm for rs-FC (*c*) and m-ISFC (*f*). The number by each bar indicates the total number of parcels contained in the cluster. Two clusters containing less than 3 parcels are not shown. (*g*) Clusters for rs-FC (left) and m-ISFC (right) were projected onto the cortical surface.

computed without assuming a predefined network structure by using the Louvain algorithm, modularity scores during rest and natural vision were roughly similar at moderate and low edge densities (Fig. 6*a*, right panel). Therefore, natural vision produced a new network organization that was roughly as modular as the organization during rest. This is consistent with the clear network organization shown in the m-ISFC matrix that was ordered by the dendrogram from the clustering analysis (Fig. 5*d*).

As in the clustering analysis, one community for m-ISFC (#1 in Fig. 6*c*) merged the visual network and the RST network involved in navigation, scene perception and scene memory (see Fig. 6*b* for the topography of each Louvain community). Similarly, the DAN was again split between 2 communities (i.e., the green blocks within clusters #5 and #6 in Figure 6*c*, right column).

Visualization of the Network Organization during Rest and Natural Vision

To illustrate the functional groupings identified by the clustering and graph analyses and to provide more insight into their

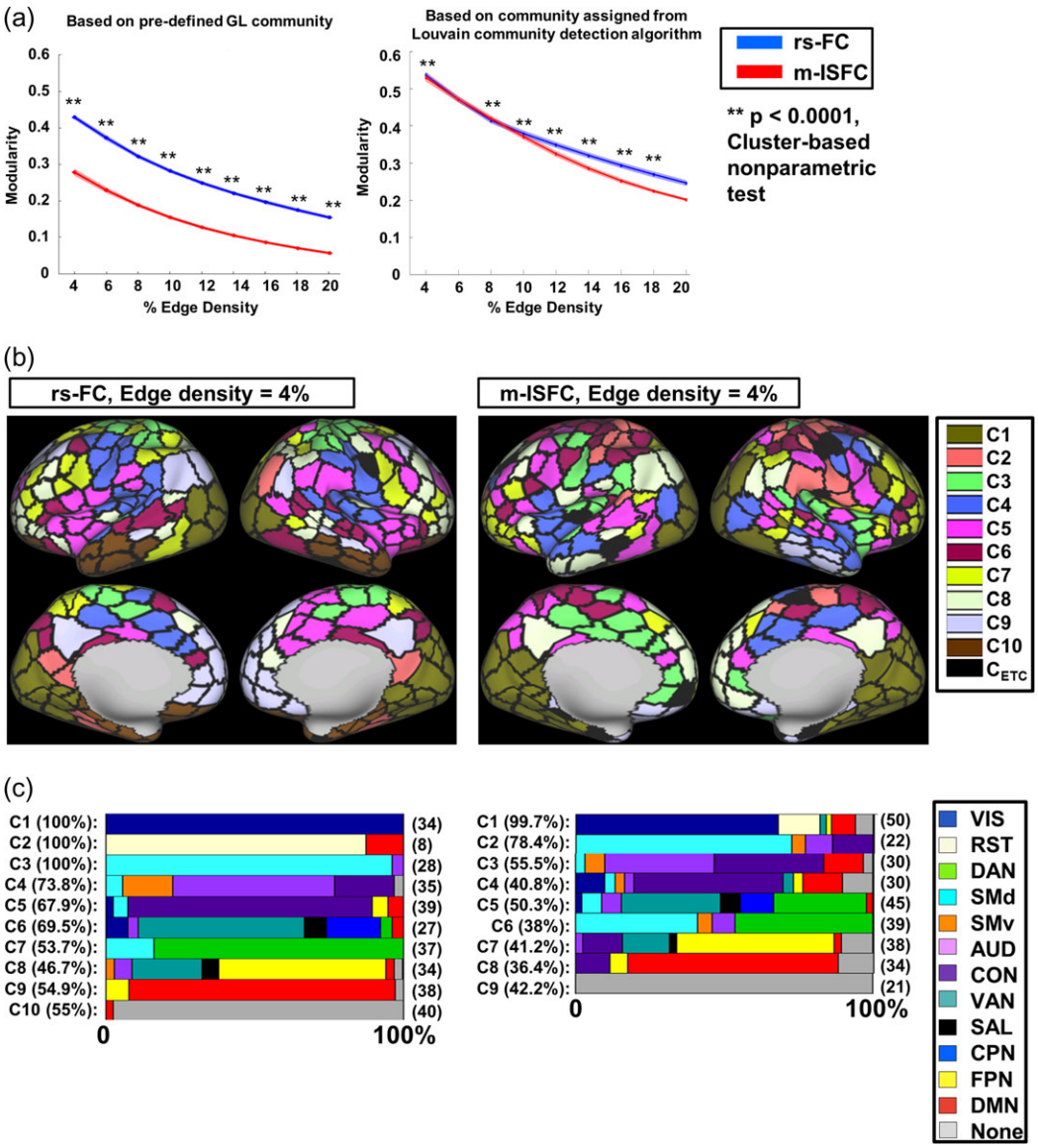

Figure 6. Analysis of community structure and modularity during rest and natural vision. (*a*) Modularity of rs-FC (blue) and m-ISFC (red) matrices was computed using the predefined Gordon–Laumann communities (left graph), or without assuming a preexisting community structure by using the Louvain algorithm (right graph). A cluster-based nonparametric test with a *P*-value of 0.0001 was performed to test for a difference in mean modularity between rs-FC and m-ISFC. (*b*) Communities identified using the Louvain algorithm (C1–C10) for rs-FC (left) and m-ISFC (right) were projected onto the cortical surface. The percentage distribution of predefined RSNs for the communities identified by the Louvain algorithm for (*c*) rs-FC and m-ISFC. The number on the right of the each bar indicates the total number of parcels contained in the community. The number on the left of the each bar indicates the frequency of community assignments from 10 000 iterations of the Louvain Algorithm. Communities containing fewer than 5 parcels are not shown.

functions, resting-state FC (rs-FC) and movie-evoked FC (m-ISFC) matrices were visualized via spring-embedded models (Fig. 7). The colors of the nodes in the models in Figure 7*a*,*d* were based on the apriori Gordon–Laumann networks, those in Figure 7*b*,*e* on the communities from the unsupervised Louvain algorithm, and those in Figure 7*c*,*f* on the top-level clusters from the hierarchical clustering analysis.

Under resting conditions, the spring-embedded model of the apriori Gordon–Laumann networks (Fig. 7*a*) was very similar to the model of the Louvain communities (Fig. 7*b*), with nodes of similar colors (i.e., nodes from similar apriori networks or Louvain communities) grouped together. Therefore, the data-driven resting network structure from the current study matched that observed in previous studies. Additionally, the spring-embedded model of rs-FC showed a similar arrangement to the spring-embedded resting-state model reported in a previous study (Power et al. 2011). Finally, the top-level grouping from the cluster analysis (Fig. 7*c*) showed a clear separation that corresponded to the distinction between internally directed and externally directed networks, again consistent with previous work (Fox et al. 2005; Golland et al. 2008).

In contrast, under natural vision the apriori Gordon–Laumann networks (Fig. 7*d*) did not match the new BOLD network structure, with intermingling of differently colored nodes to form new functional groupings. These groupings, presumably adaptive for natural vision, are evident in Figure 7*e*,*f*, which display respectively the Louvain communities and the top-level clusters from the clustering analysis. The visual and

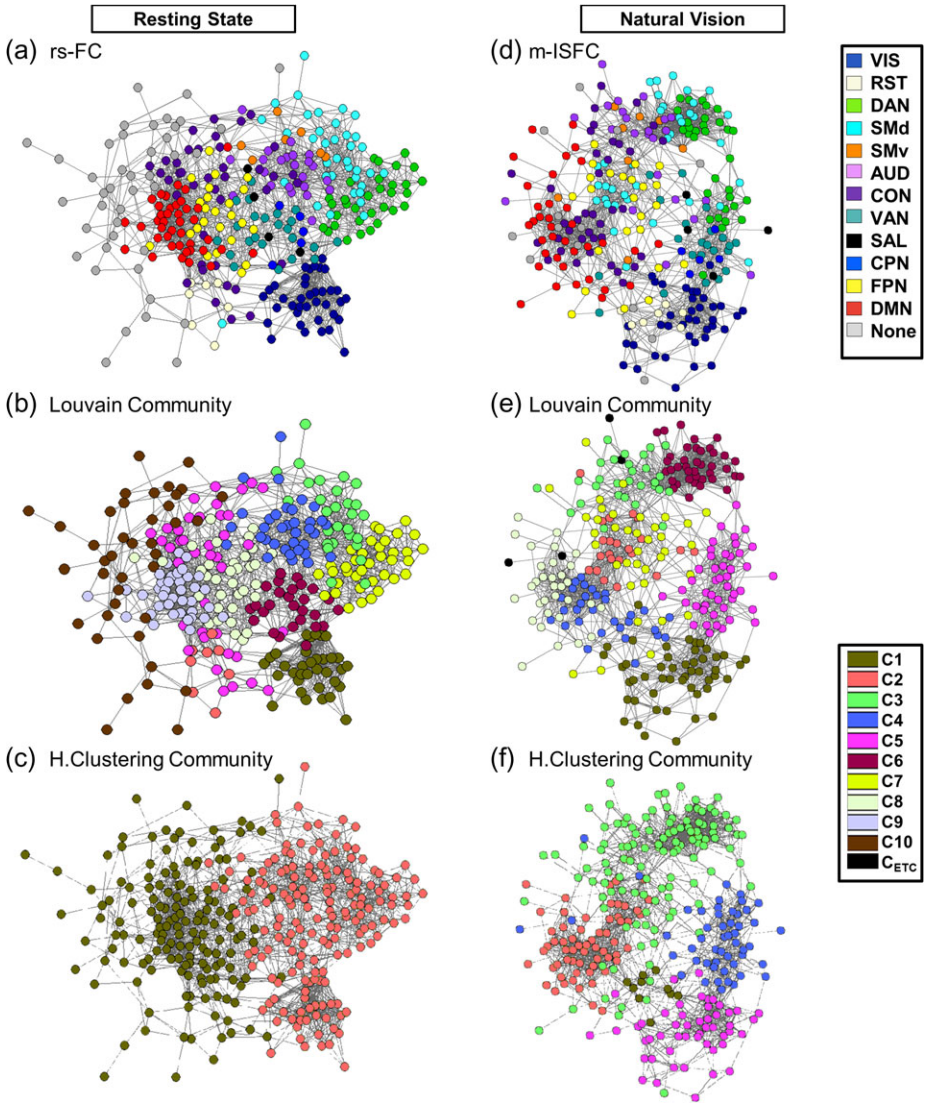

Figure 7. Spring-embedded models reveal different network organizations for rest and natural vision. Spring-embedded models were generated for resting-state FC (rs-FC) and movie-evoked FC (m-ISFC) matrices of 4% edge density. Nodes were colored by the predefined network assignment from the Gordon–Laumann parcellation (*a*,*d*), by Louvain community assignment (*b*,*e*), and by Hierarchical clustering (*c*,*f*). See Figures 5*c*,*f* and 6*c* for the percentage distribution of predefined RSNs for each cluster and community.

RST network were merged into a single vision/scene analysis community (community #1, Fig. 7*e*; also cluster #5, Fig. 7*f*), as noted earlier, which was adjacent to a community (#5, Fig. 7*e*; also cluster #4, Fig. 7*f*) that combined more visually related parcels from the DAN and VAN/language parcels (see Fig. 7*d*). The DAN/VAN component of this multicommunity grouping might be involved in controlling attention to the display. The remaining parcels of the DAN were integrated with many dorsal somatomotor parcels (Fig. 7*d*) into Community #6, which was adjacent to a community (#3, Fig. 7*e*) containing many parcels from the auditory network (Fig. 7*d*). This DAN/SMd/AUD grouping could reflect attention to/interpretation of action as well as sound, perhaps including dialog. Community #7 (Fig. 7*e*) was possibly the most centrally located in the model and primarily contained parcels from the FPN, along with small contributions from the VAN and CON. The central location of this "cognitive control" community was consistent with the critical role of the FPN in task-dependent processing (Dosenbach et al. 2008; Cole et al. 2013).

Discussion

Natural vision produced substantial modifications in the FC observed at rest, resulting in a new BOLD network structure that was roughly as modular as the resting structure. During natural vision, RSNs were split into components that recombined with components from other RSNs to form new communities, or remained intact but merged with other RSNs to form larger communities. As discussed below, the formation of these communities was consistent with the cognitive demands imposed by natural vision. Interestingly, these groupings did not necessarily respect the large-scale internal/external distinction that governs resting-state structure, indicating a fundamental change from the resting structure. All of the above results were supported by both hierarchical clustering and graph-based analyses and indicate that the BOLD network structure evoked by natural vision was only partly constrained by the resting structure.

BOLD Network Organization during Natural Vision and Rest

Movie viewing changed the network structure observed during rest to produce new functional groupings in line with the demands of natural vision. The visual network merged with the network for navigation, scene perception and scene memory, along with parcels from the FPN to form a community adaptive for analyzing the visual content of the movie. The dorsal attention network was split into 2 parts that may have reflected the multimodal/multidimensional nature of the movie. Parcels from the DAN and VAN, along with some from the salience and cingulo-parietal networks, were combined into a single community that was adjacent to the visual/scene community described above. This larger DAN/VAN/VIS/Scene grouping may have been involved in controlling attention to the display. The remaining DAN parcels were integrated with dorsal somato-motor parcels into a community adjacent to another community that included large contributions from the auditory network. The resulting DAN/SMd/AUD grouping may have been involved in attention to/interpretation of action and perhaps attention to sound and dialog. Although these assignments of function are speculative, the reorganization of the dorsal attention network into 2 separate communities/clusters was evident both in the Louvain community analyses and in the cluster analysis. Finally, internally- and externally-directed processes interacted more strongly during natural vision than rest. The DBI for resting FC showed a minimum at 2 clusters, and the composition of those clusters matched the internal/external distinction. In contrast, the smallest local minimum value of the DBI for natural vision occurred at seven clusters, and the largest cluster found combined parcels from several internal and external networks. Similarly, Louvain communities combined CON parcels with those from the auditory network and dorsal somato-motor network.

The observed changes in BOLD network structure were consistent with prior observations of differences in FC during resting and task states. Spadone et al. reported increased FC between visual and dorsal attention regions during an attention-shifting paradigm (Spadone et al. 2015). Betti et al. reported with fMRI and MEG a decrease in the correlation within networks of alpha/beta band limited power (BLP, especially visual and auditory), and an increase in the correlation between networks (e.g., visual and language networks) of theta, beta, and gamma BLP (Betti et al. 2013). Both Spadone et al. and Betti et al. reported that the overall topographies of FC during rest and natural vision were very similar, as did a subsequent fMRI paper by Cole et al. (2014), but their methodologies did not remove the effects of intrinsic activity during movie viewing (see below, relation to previous studies).

Implications for the Function of Resting-State Activity

The introduction noted 2 different conceptions of the relationship between intrinsic and task-evoked activity, that is, a task state is selected from a broad repertoire of resting states or is independently generated from a default resting state through unknown mechanisms. The new BOLD network organization observed during natural vision seems more consistent with the latter viewpoint, a conclusion similar to that of Betti et al. (2013). Our results indicate that resting state organization does not fully constrain the large-scale FC of brain areas that is adaptive for natural vision. More generally, we suggest that the brain can change its network structure to meet the demands of a task even if that structure departs substantially from the resting structure. The view that network structure can change to meet the current task demand is in line with previous views (Miller and Cohen 2001; Heinzle et al. 2012).

Sources of the Residual Shared Structure Between Rest and Task

Although the spatial correlation between rest and movie, $r = 0.60$, was smaller than the rest–task correlations previously reported, it was nonetheless significant. This result is, consistent with recent studies indicating that task activation can be predicted from resting FC (Cole et al. 2016; Tavor et al. 2016). Importantly, since the ISFC procedure completely removed the effects of intrinsic activity from the FC matrix, the shared FC topography did not reflect a common source of signals, that is, intrinsic activity, but instead represented a correspondence between the resting network structure and the evoked structure observed during natural vision. A focus on this residual correspondence may allow a better understanding of how resting-state FC constrains task-evoked signals and FC.

This correspondence may have resulted from several factors. First, a common structural connectivity matrix promotes rest–task correspondence (Vincent et al. 2006; Greicius et al. 2009; Hasson et al. 2009; Honey et al. 2009). Bartfeld et al. studied the variability of FC whole brain patterns in different behavioral conditions (awake, drowsy, anesthesia) in monkeys (Barttfeld et al. 2015). They reported that the variability of FC patterns increased with arousal/wakefulness, and that FC patterns under anesthesia were closely related to the structural connectivity organization. The latter, structurally driven component of FC should be common to task and rest.

In addition, experience driven by natural vision may include some modal or highly frequent FC patterns that through repetition and Hebbian mechanisms become part of the tonic, resting FC structure. Consistent with this idea several studies have reported modifications of resting FC patterns after learning (Albert et al. 2009; Lewis et al. 2009; Tambini et al. 2010; Harmelech and Malach 2013). Recent work has also suggested long-term, experience-dependent influences on FC in visual cortex. FC between different visual areas is increased in ROIs that have overlapping receptive fields (Heinzle et al. 2011; Raemaekers et al. 2014; Wilf et al. 2017) or represent similar eccentricities (Arcaro et al. 2015). Wilf et al. (2017) additionally reported that the FC of visual cortex from movie viewing, after removal of intrinsic activity, was more similar to resting FC than the FC from iso-eccentricity stimulation, iso-polar stimulation, or predictions based on retinotopic, polar angle or eccentricity distance. Therefore, a component of the residual shared structure between rest and natural vision likely reflects frequently experienced patterns of interregional, evoked activity. Conversely, the FC in visual cortex evoked by stimulation can differ from resting FC, with larger differences for nonnaturalistic stimulation.

Finally, FC on average is greater between nearby brain regions both during task and rest, an effect that largely reflects stronger structural and functional interactions between neighboring regions, but may also partly result from method-related factors such as smoothing.

Relation to Previous Studies

The conclusion that natural vision produced large changes in the resting network structure does not conflict with the

previous results of Cole et al., who reported very similar FC matrices for resting and task conditions, since the latter authors did not remove the effects of intrinsic activity from their task FC matrices (Cole et al. 2014). Interestingly, Cole et al. also reported that regressing the mean task activity from the BOLD time series only slightly increased the correlation of rest and task FC matrices from 0.86 to 0.90 (results taken from the HCP "seven-task" dataset, $n = 118$). The large effect of removing intrinsic activity on the movie FC matrix, coupled with the much smaller effect of removing mean task activity on the task FC matrix (Cole et al. 2014), suggests that intrinsic fluctuations are larger in magnitude than task/movie-evoked fluctuations. On this view, the resting FC matrix matched the nonregressed task FC matrix in Cole et al. and the movie FC matrix (m-FC) in the present study because during the task/movie the sum of the intrinsic modulations and the (very different) task/movie-evoked modulations was dominated by the same intrinsic modulations that were present at rest.

The same factor, in conjunction with the insensitivity of correlation to overall changes in magnitude, explains why the intersubject averaging and ISFC procedures produced very similar movie FC matrices but very different resting FC matrices. Intersubject averaging of intrinsic fluctuations greatly reduced their magnitude. As a result, the sum of these signals with the movie-evoked signals was dominated by the latter, producing similar m-avg and m-ISFC matrices. However, during rest the intrinsic signals were not summed with signals from a different source. Therefore, smaller amplitude intrinsic signals were sufficient to produce the same FC matrix as the resting matrix measured without intersubject averaging. Larger amplitudes of intrinsic than movie-evoked activity might partly reflect the fact that the power of the local field potential is on average greater and more synchronized at rest than during tasks (Pfurtscheller and Lopes da Silva 1999; Betti et al. 2013).

Group FC Versus Subject-Specific FC

The ISFC procedure (Simony et al. 2016) is a powerful technique for eliminating the influence of intrinsic activity on the FC measured during a task. It produces stable estimates of FC, uncontaminated by intrinsic activity, over a wide range of sample sizes. In contrast, the temporal averaging procedure requires a large sample size to achieve a similar result. It is important to note, however, that the ISFC procedure as well as temporal averaging also eliminates task-evoked FC that is specific to an individual rather than common across a group.

Wilf et al. (2017) have reported a procedure that eliminates the effects of intrinsic signals on FC while retaining both group and subject-specific, movie-evoked FC. Their subjects viewed the same movie twice, allowing within-subject FC to be computed from the correlation between the 2 viewings (see Henrikksen et al. for a related approach in which representational dissimilarity matrices were computed within versus across trials, and Hasson et al. for earlier work on intersubject synchronization during movie viewing). However, this procedure only preserved group and individual FC patterns that were invariant over repeated viewings, which could skew the observed FC. For example, on a second viewing, subjects likely could better predict the spatio-temporal content of the movie.

Limitations

Because eye movements are not controlled in the natural vision paradigm each subject may have received different retinal inputs during the movie, depending on their fixation patterns. As noted above, subject-specific FC was not assessed by the ISFC technique. However, the free-viewing paradigm has been used in many previous fMRI studies of natural vision (Hasson et al. 2004; Bartels and Zeki 2005; Golland et al. 2008; Huth et al. 2012; Mantini et al. 2012; Betti et al. 2013; Stansbury et al. 2013) and has consistently shown strong intersubject correlations in visual cortex as well as many other brain regions (Hasson et al. 2004, 2010). Responses in visual cortex are sufficiently consistent that a reverse inference procedure can be conducted in which the brain response in a region such as the fusiform gyrus during individual frames of the movie can be used to predict the regions' selectivity (Hasson et al. 2004). In the current paper, the m-ISFC matrix showed high correlations between visual regions. Therefore, movie-viewing evokes a consistent BOLD response across many brain regions, despite the fact that eye movements are not controlled. In this paper, we studied the network organization over the entire brain of these consistent responses.

Because the present work was based on the BOLD signal, our conclusions only apply to low-frequency activity. Although the relationship between FC networks during task and rest has been measured at higher frequencies (Betti et al. 2013), intrinsic signals were not removed from task FC.

m-ISFC reflects an unknown mixture of interregional interactions and independent coactivations. Although Cole et al. (2014) removed the mean BOLD activation from task time series through regression, an analogous procedure was not possible here since the movie did not involve repeated "trials," that is, each time segment of the movie was different.

The ISFC procedure eliminates interactions between task-evoked signals and intrinsic signals, treating these signals as additive. Some prior studies reporting high task-rest similarity used procedures that also likely minimized or attenuated interaction effects, suggesting that these effects do not explain the reduction of task-rest similarity when intrinsic activity is removed. The high correspondence reported by Smith et al. (2009), for example, was not caused by interactions, since time-locked activations have no consistent phase relationship with intrinsic activity. Cole et al. (2014) compared the similarity of group-averaged task-evoked FC matrices with group-averaged resting FC matrices rather than calculating task-rest similarity in individuals. Group-averaging would have minimized interaction effects that differed across subjects. Moreover, the effects of interactions on the similarity of task-evoked and resting FC may depend on the detailed nature and consistency of the interactions across regions, and therefore may be difficult to predict. However, we acknowledge that interactions between task-evoked signals and intrinsic activity may well affect task-rest similarity and consequently the degree to which reductions are observed when intrinsic activity is removed.

The reduction in movie-rest similarity after the effects of intrinsic activity were removed was highly robust and consistent across individual movies. One question, however, is whether similar reductions will be found for other kinds of tasks. The seven tasks from the Human Connectome dataset tested by Cole et al. (2014), Emotional, Gambling, Language, Motor, Relational, Social, and N-back, showed correlation coefficients between rest and task FC matrices that were very similar to those between rest and m-FC matrices (i.e., matrices in which the effects of intrinsic activity were not removed), with only modest variation across the seven tasks ($\mu = 0.83$, $\sigma = 0.037$). However, despite the similarity of rest–task correspondences across movies and tasks when intrinsic activity was left

in, it is still possible that the magnitude of reductions in similarity when intrinsic activity is removed will differ for some tasks.

Finally, although the relationship between resting and task-evoked activity has usually been conceptualized in terms of the correspondence between resting and task networks defined by interregional correlations or between resting networks and patterns of task coactivation, it also can be conceptualized in terms of the similarity of the information carried by patterns of neural activity during task and rest (Fiser et al. 2010). Numerous studies have shown that multivoxel patterns of local activity during tasks carry information about specific stimuli, classes of stimuli, or even task operations (Haxby et al. 2001; Kamitani and Tong 2005; Haynes and Rees 2006; Kriegeskorte et al. 2008; Connolly et al. 2012; Guntupalli et al. 2016), and can be modulated by learning and attention. The current study, however, did not test whether intrinsic activity influences or constrains the information carried by task-evoked activity since activity was averaged over a parcel and was not analyzed using multivoxel techniques.

Supplementary Material

Supplementary data are available at *Cerebral Cortex* online.

Funding

This work was supported by the National Institutes of Health (RO1 MH096482 and NS095741).

Notes

We thank Davis Van Essen, Matt Glasser, and Tim Brown for providing HCP Minimum Pipeline Preprocessed HCP 7 T fMRI data, and thank for all people involved in HCP-consortium. In addition, we thank Joshua Siegel for help with the graph-theory analyses. *Conflict of Interest*: None declared.

References

Albert NB, Robertson EM, Miall RC. 2009. The resting human brain and motor learning. Curr Biol. 19(12):1023–1027.

Arcaro MJ, Honey CJ, Mruczek RE, Kastner S, Hasson U. 2015. Widespread correlation patterns of fMRI signal across visual cortex reflect eccentricity organization. Elife. 19:4.

Bartels A, Zeki S. 2005. Brain dynamics during natural viewing conditions—a new guide for mapping connectivity in vivo. Neuroimage. 24(2):339–349.

Barttfeld P, Uhrig L, Sitt JD, Sigman M, Jarraya B, Dehaene S. 2015. Signature of consciousness in the dynamics of resting-state brain activity. Proc Natl Acad Sci USA. 112(3):887–892.

Becker R, Reinacher M, Freyer F, Villringer A, Ritter P. 2011. How ongoing neuronal oscillations account for evoked fMRI variability. J Neurosci. 31(30):11016–11027.

Berkes P, Orban G, Lengyel M, Fiser J. 2011. Spontaneous cortical activity reveals hallmarks of an optimal internal model of the environment. Science. 331(6013):83–87.

Betti V, DellaPenna S, de Pasquale F, Mantini D, Marzetti L, Romani GL, Corbetta M. 2013. Natural scenes viewing alters the dynamics of functional connectivity in the human brain. Neuron. 79(4):782–797.

Biswal B, Yetkin FZ, Haughton VM, Hyde JS. 1995. Functional connectivity in the motor cortex of resting human brain using echo-planar MRI. Magn Reson Med. 34(4):537–541.

Blondel VD, Guillaume JL, Lambiotte R, Lefebvre E. 2008. Fast unfolding of communities in large networks. J Stat Mech. 2008:1–12.

Brookes MJ, Woolrich M, Luckhoo H, Price D, Hale JR, Stephenson MC, Barnes GR, Smith SM, Morris PG. 2011. Investigating the electrophysiological basis of resting state networks using magnetoencephalography. Proc Natl Acad Sci USA. 108(40):16783–16788.

Cauda F, Costa T, Diano M, Sacco K, Duca S, Geminiani G, Torta DM. 2014. Massive modulation of brain areas after mechanical pain stimulation: a time-resolved FMRI study. Cereb Cortex. 24(11):2991–3005.

Cole MW, Bassett DS, Power JD, Braver TS, Petersen SE. 2014. Intrinsic and task-evoked network architectures of the human brain. Neuron. 83(1):238–251.

Cole MW, Ito T, Bassett DS, Schultz DH. 2016. Activity flow over resting-state networks shapes cognitive task activations. Nat Neurosci. 19(12):1718–1726.

Cole MW, Reynolds JR, Power JD, Repovs G, Anticevic A, Braver TS. 2013. Multi-task connectivity reveals flexible hubs for adaptive task control. Nat Neurosci. 16(9):1348–1355.

Connolly AC, Guntupalli JS, Gors J, Hanke M, Halchenko YO, Wu YC, Abdi H, Haxby JV. 2012. The representation of biological classes in the human brain. J Neurosci. 32(8):2608–2618.

Cordes D, Haughton VM, Arfanakis K, Carew JD, Turski PA, Moritz CH, Moritz CH, Quigley MA, Meyerand ME. 2001. Frequencies contributing to functional connectivity in the Cereb Cortex. in "resting-state" data. Am J Neuroradiol. 22 (7):1326–1333.

Davies DL, Bouldin DW. 1979. A cluster separation measure. IEEE Trans Pattern Anal Mach Intell. 1(2):224–227.

de Pasquale F, Della Penna S, Snyder AZ, Lewis C, Mantini D, Marzetti L, Belardinelli P, Ciancetta L, Pizzella V, Romani GL, et al. 2010. Temporal dynamics of spontaneous MEG activity in brain networks. Proc Natl Acad Sci USA. 107(13): 6040–6045.

Dosenbach NU, Fair DA, Cohen AL, Schlaggar BL, Petersen SE. 2008. A dual-networks architecture of top-down control. Trends Cogn Sci. 12(3):99–105.

Fiser J, Berkes P, Orbán G, Lengyel M. 2010. Statistically optimal perception and learning:from behavior to neural representations. Trends Cogn Sci. 14(3):119–130.

Fiser J, Chiu C, Weliky M. 2004. Small modulation of ongoing cortical dynamics by sensory input during natural vision. Nature. 431(7009):573–578.

Florin E, Baillet S. 2015. The brain's resting-state activity is shaped by synchronized cross-frequency coupling of oscillatory neural activity. Neuroimage. 111:26–35.

Fox MD, Snyder AZ, Vincent JL, Corbetta M, Van Essen DC, Raichle ME. 2005. The human brain is intrinsically organized into dynamic, anticorrelated functional networks. Proc Natl Acad Sci USA. 102(27):9673–9678.

Fox MD, Snyder AZ, Zacks JM, Raichle ME. 2006. Coherent spontaneous activity accounts for trial-to-trial variability in human evoked brain responses. Nat Neurosci. 9(1):23–25.

Glasser MF, Sotiropoulos SN, Wilson JA, Coalson TS, Fisch B, Andersson JL, Xu J, Jbabdi S, Webster M, Polimeni JR, et al. 2013. The minimal preprocessing pipelines for the Human Connectome Project. Neuroimage. 80:105–124.

Golland Y, Golland P, Bentin S, Malach R. 2008. Data-driven clustering reveals a fundamental subdivision of the human cortex into two global systems. Neuropsychologia. 46(2): 540–553.

Gordon EM, Laumann TO, Adeyemo B, Huckins JF, Kelley WM, Petersen SE. 2016. Generation and evaluation of a cortical area parcellation from resting-state correlations. Cereb Cortex. 26(1):288–303.

Greicius MD, Supekar K, Menon V, Dougherty RF. 2009. Resting-state functional connectivity reflects structural connectivity in the default mode network. Cereb Cortex. 19(1):72–78.

Guntupalli JS, Hanke M, Halchenko YO, Connolly AC, Ramadge PJ, Haxby JV. 2016. A model of representational spaces in human cortex. Cereb Cortex. 26(6):2919–2934.

Harmelech T, Malach R. 2013. Neurocognitive biases and the patterns of spontaneous correlations in the human cortex. Trends Cogn Sci. 17(12):606–615.

Hasson U, Malach R, Heeger DJ. 2010. Reliability of cortical activity during natural stimulation. Trends Cogn Sci. 14(1): 40–48.

Hasson U, Nir Y, Levy I, Fuhrmann G, Malach R. 2004. Intersubject synchronization of cortical activity during natural vision. Science. 303(5664):1634–1640.

Hasson U, Nusbaum HC, Small SL. 2009. Task-dependent organization of brain regions active during rest. Proc Natl Acad Sci USA. 106(26):10841–10846.

Haxby JV, Gobbini MI, Furey ML, Ishai A, Schouten JL, Pietrini P. 2001. Distributed and overlapping representations of faces and objects in ventral temporal cortex. Science. 293(5539): 2425–2430.

Haynes JD, Rees G. 2006. Decoding mental states from brain activity in humans. Nat Rev Neurosci. 7(7):523–534.

He BJ, Snyder AZ, Zempel JM, Smyth MD, Raichle ME. 2008. Electrophysiological correlates of the brain's intrinsic large-scale functional architecture. Proc Natl Acad Sci USA. 105(41): 16039–16044.

Heinzle J, Kahnt T, Haynes JD. 2011. Topographically specific functional connectivity between visual field maps in the human brain. Neuroimage. 56(3):1426–1436.

Heinzle J, Wenzel MA, Haynes JD. 2012. Visuomotor functional network topology predicts upcoming tasks. J Neurosci. 32(29): 9960–9968.

Henriksson L, Khaligh-Razavi SM, Kay K, Kriegeskorte N. 2015. Visual representations are dominated by intrinsic fluctuations correlated between areas. Neuroimage. 114:275–286.

Honey CJ, Sporns O, Cammoun L, Gigandet X, Thiran JP, Meuli R, Hagmann P. 2009. Predicting human resting-state functional connectivity from structural connectivity. Proc Natl Acad Sci USA. 106(6):2035–2040.

Huth AG, Nishimoto S, Vu AT, Gallant JL. 2012. A continuous semantic space describes the representation of thousands of object and action categories across the human brain. Neuron. 76(6):1210–1224.

Kamitani Y, Tong F. 2005. Decoding the visual and subjective contents of the human brain. Nat Neurosci. 8(5):679–685.

Kenet T, Bibitchkov D, Tsodyks M, Grinvald A, Arieli A. 2003. Spontaneously emerging cortical representations of visual attributes. Nature. 425(6961):954–956.

Kriegeskorte N, Mur M, Ruff DA, Kiani R, Bodurka J, Esteky H, Tanaka K, Bandettini PA. 2008. Matching categorical object representations in inferior temporal cortex of man and monkey. Neuron. 60(6):1126–1141.

Laumann TO, Gordon EM, Adeyemo B, Synder AZ, Joo SJ, Chen MY, Gilmore AW, McDermott KB, Nelson SM, Dosenbach NU, et al. 2015. Functional system and areal organization of a highly sampled individual human brain. Neuron. 87(3): 657–670.

Lewis CM, Baldassarre A, Committeri G, Romani GL, Corbetta M. 2009. Learning sculpts the spontaneous activity of the resting human brain. Proc Natl Acad Sci USA. 106(41):17558–17563.

Mantini D, Hasson U, Betti V, Perrucci MG, Romani GL, Corbetta M, Orban GA, Vanduffel W. 2012. Interspecies activity correlations reveal functional correspondence between monkey and human brain areas. Nat Methods. 9(3):277–282.

Maris E, Oostenveld R. 2007. Nonparametric statistical testing of EEG- and MEG-data. J Neurosci Methods. 164(1):177–190.

Mennes M, Kelly C, Colcombe S, Castellanos FX, Milham MP. 2013. The extrinsic and intrinsic functional architectures of the human brain are not equivalent. Cereb Cortex. 23(1): 223–229.

Miller EK, Cohen JD. 2001. An integrative theory of prefrontal cortex function. Annu Rev Neurosci. 24:167–202.

Newman ME. 2004. Fast algorithm for detecting community structure in networks. Phys Rev E Stat Nonlin Soft Matter Phys. 69(6 Pt 2):066133.

Newman ME, Girvan M. 2004. Finding and evaluating community structure in networks. Phys Rev E Stat Nonlin Soft Matter Phys. 69(2 Pt 2):026113.

Nir Y, Mukamel R, Dinstein I, Privman E, Harel M, Fisch L, Gelbard-Sagiv H, Kipervasser S, Andelman F, Neufeld MY, et al. 2008. Interhemispheric correlations of slow spontaneous neuronal fluctuations revealed in human sensory cortex. Nat Neurosci. 11(9):1100–1108.

Petersen SE, Sporns O. 2015. Brain networks and cognitive architectures. Neuron. 88(1):207–219.

Pfurtscheller G, Lopes da Silva FH. 1999. Event-related EEG/MEG synchronization and desynchronization:Basic principles. Clin Neurophysiol. 110(11):1842–1857.

Power JD, Barnes KA, Snyder AZ, Schlaggar BL, Petersen SE. 2012. Spurious but systematic correlations in functional connectivity MRI networks arise from subject motion. NeuroImage. 59(3):2142–2154.

Power JD, Cohen AL, Nelson SM, Wig GS, Barnes KA, Church JA, Vogel AC, Laumann TO, Miezin FM, Schlaggar BL, et al. 2011. Functional network organization of the human brain. Neuron. 72(4):665–678.

Prichard D, Theiler J. 1994. Generating surrogate data for time series with several simultaneously measured variables. Phys Rev Lett. 73(7):951–954.

Raemaekers M, Schellekens W, van Wezel RJ, Petridou N, Kristo G, Ramsey NF. 2014. Patterns of resting state connectivity in human primary visual cortical areas: a 7 T fMRI study. Neuroimage. 84:911–921.

Raichle ME. 2011. The restless brain. Brain Connect. 1(1):3–12.

Riedel MC, Ray KL, Dick AS, Sutherland MT, Hernandez Z, Fox PM, Eickhoff SB, Fox PT, Laird AR. 2015. Meta-analytic connectivity and behavioral parcellation of the human cerebellum. Neuroimage. 117:327–342.

Rubinov M, Sporns O. 2010. Complex network measures of brain connectivity: uses and interpretations. NeuroImage. 52(3):1059–1069.

Simony E, Honey CJ, Chen J, Lositsky O, Yeshurun Y, Wiesel A, Hasson U. 2016. Dynamical reconfiguration of the default mode network during narrative comprehension. Nat Commun. 7:12141.

Smith SM, Fox PT, Miller KL, Glahn DC, Fox PM, Mackay CE, Filippini N, Watkins KE, Toro R, Laird AR, et al. 2009. Correspondence of the brain's functional architecture during activation and rest. Proc Natl Acad Sci USA. 106(31): 13040–13045.

Spadone S, Della Penna S, Sestieri C, Betti V, Tosoni A, Perrucci MG, Romani GL, Corbetta M. 2015. Dynamic reorganization of human resting-state networks during visuospatial attention. Proc Natl Acad Sci USA. 112(26):8112–8117.

StansburyDENaselarisTGallantJL2013Natural scene statistics account for the representation of scene categories in human visual cortexNeuron79510251034

Tambini A, Ketz N, Davachi L. 2010. Enhanced brain correlations during rest are related to memory for recent experiences. Neuron. 65(2):280–290.

Tavor I, Parker Jones O, Mars RB, Smith SM, Behrens TE, Jbabdi S. 2016. Task-free MRI predicts individual differences in brain activity during task performance. Science. 352(6282):216–220.

Tsodyks M, Kenet T, Grinvald A, Arieli A. 1999. Linking spontaneous activity of single cortical neurons and the underlying functional architecture. Science. 286(5446):1943–1946.

Uğurbil K, Xu J, Auerbach EJ, Moeller S, Vu AT, Duarte-Carvajalino JM, Lenglet C, Wu X, Schmitter S, Van de Moortele PF, et al. 2013. Pushing spatial and temporal resolution for functional and diffusion MRI in the Human Connectome Project. NeuroImage. 80:80–104.

Van Essen DC, Ugurbil K, Auerbach E, Barch D, Behrens TEJ, Bucholz R, Chang A, Chen L, Corbetta M, Curtiss SW, et al. 2012. The human connectome project: a data acquisition perspective. NeuroImage. 62(4):2222–2231.

Varela F, Lachaux JP, Rodriguez E, Martinerie J. 2001. The brainweb: phase synchronization and large-scale integration. Nat Rev Neurosci. 2(4):229–239.

Vincent JL, Snyder AZ, Fox MD, Shannon BJ, Andrews JR, Raichle ME, Buckner RL. 2006. Coherent spontaneous activity identifies a hippocampal-parietal memory network. J Neurophysiol. 96(6):3517–3531.

Wilf M, Strappini F, Golan T, Hahamy A, Harel M, Malach R. 2017. Spontaneously emerging patterns in human visual cortex reflect responses to naturalistic sensory stimuli. Cereb Cortex. 27(1):750–763.